# Morphology and Biodegradability of Poly(ε-caprolactone)/Poly(vinyl alcohol) Block Copolymers

Jin Zhou, Yoshiro Nishimura, Akinori Takasu, Yoshihito Inai, and Tadamichi Hirabayashi[†]

*Department of Environmental Technology and Urban Planning, Graduate School of Engineering,*
*Nagoya Institute of Technology, Gokiso-cho, Showa-ku, Nagoya 466-8555, Japan*

ABSTRACT: Poly(ε-caprolactone)-*block*-poly(vinyl alcohol) (PCL-*b*-PVA) copolymers were prepared by using a bifunctional initiator 4-(2-hydroxyethoxy)-benzaldehyde (4-HEBA), which could respond to both ring-opening polymerization and aldol-type group transfer polymerization. Morphological changes along with block length ratios were observed with differential scanning calorimeter and polarized optical microscope. Increment of PVA block influenced the crystallizing manner of PCL block. Biodegradability of PCL-*b*-PVA copolymers, two homopolymers (PCL and PVA), and PCL/PVA blend was evaluated from biochemical oxygen demand (BOD) in the presence of activated sludge. Under the conditions in this study, the biodegradation behavior of PCL-*b*-PVA copolymer was influenced by shape of sample. Increment of the PVA block in PCL-*b*-PVA copolymers slowed down biodegradation rates. When the content of PVA block in the block copolymer increased to more than 25 mol %, the biodegradation of PCL moiety was effectively inhibited even after much longer exposure time. [DOI 10.1295/polymj.36.695]
KEY WORDS Poly(ε-caprolactone)-*block*-Poly(vinyl alcohol) (PCL-*b*-PVA) / Polarized Optical Microscope / Differential Scanning Calorimeter / Morphology / Biodegradability / Biochemical Oxygen Demand (BOD) /

In the last two decades, numerous biodegradable polymers have been developed as not only environmental friendly materials but biomedical materials, such as biomedical implants, controlled drug-delivery systems, and surgical sutures. Aliphatic polyesters are the most commonly used polymers in ecological and biomedical (or pharmacological) applications, mainly due to potential for providing controlled biodegradability.[1] Among conventional aliphatic polyesters, poly(ε-caprolactone) (PCL) can be synthesized easily by ring-opening polymerization (ROP) of ε-caprolactone (ε-CL) in a living manner and is an attractive thermoplastic polymer for ecological and biomedical applications. However, its low melting point near to 60 °C limits more extensive application.
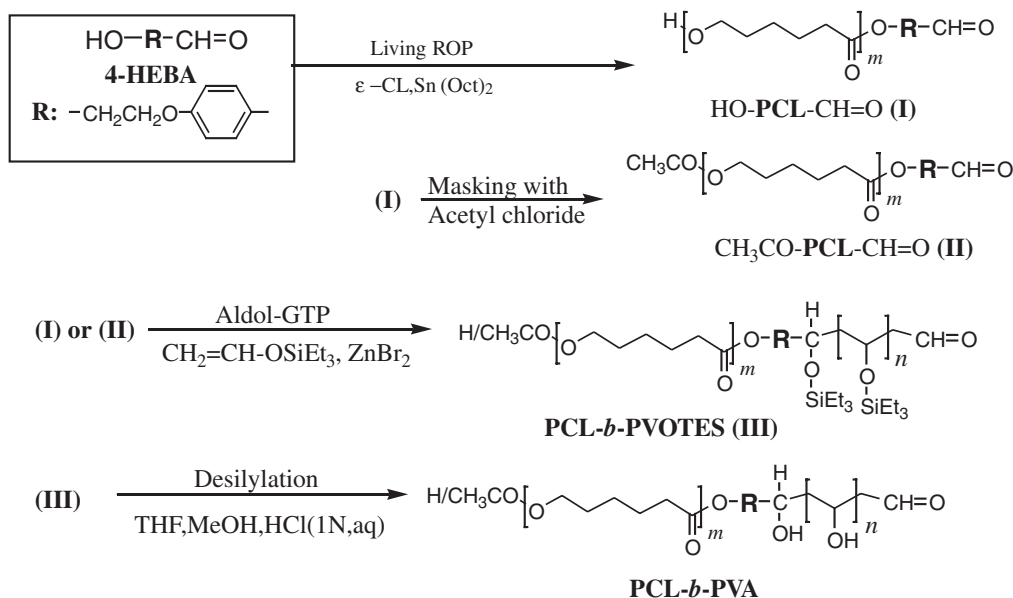
Many trials to blend or copolymerize PCL with other polymers have been carried out to raise melting temperature of the hybrid system, keeping its biodegradability. Blending is a relatively simple and easy method in comparison with building copolymers. Many blends containing PCL have been reported, for example, isotactic poly(3-hydrxy butyrate)/PCL,[2,3] poly(hydroxyl butyrate-*co*-hydroxyl valerate)/PCL,[4] poly(vinyl alcohol)/PCL,[5] poly(L-lactide)/PCL,[6] and so forth. The miscibility of components should be a key factor in determining the properties of these blends.

The development of copolymerization techniques has provided us many new PCL-based copolymers with excellent physical properties that could not be achieved through simple blending. For example, poly(L-lactide) (PLLA) having a high molecular weight is immiscible with PCL even at molten temperature and the morphology of PLLA/PCL blend becomes coarse so that desirable mechanical properties may not be expected. PLLA-*b*-PCL copolymers have various micro-domains depending on block length. Mechanical properties as well as biodegradability may be decided by micro-domain structures.[7] The biodegradation behavior of a copolymer is influenced by not only the original biodegradability of components but morphological specifications which must be determined by many secondary factors.

Diblock copolymer consisting of two chemically different polymer chains can be phase-separated, resulting in different morphological structures depending on sequence length of each block.[8] Amphiphilic block copolymers having water soluble blocks incorporated into biodegradable hydrophobic block attract our attention due to their outstanding effects as carriers for building novel drug delivery systems.[9] Poly-(ethylene oxide) (PEO) has been extensively employed as a hydrophilic polymeric component because of its excellent physicochemical and biological properties that include solubility in water and organic solvent, lack of toxicity, absence of antigenicity and immunogenicity, and filterability through the kidney at

---

[†]To whom correspondence should be addressed (E-mail: hirabaya@mse.nitech.ac.jp).

HO—**R**–CH=O
**4-HEBA**
**R:** −CH$_2$CH$_2$O—⟨benzene ring⟩—

Living ROP
$\varepsilon$–CL, Sn (Oct)$_2$
→

H–[O–(CH$_2$)$_5$–C(=O)]$_m$–O–**R**–CH=O
HO-**PCL**-CH=O (**I**)

(**I**) $\xrightarrow{\text{Masking with Acetyl chloride}}$ CH$_3$CO–[O–(CH$_2$)$_5$–C(=O)]$_m$–O–**R**–CH=O
CH$_3$CO-**PCL**-CH=O (**II**)

(**I**) or (**II**) $\xrightarrow[\text{CH}_2\text{=CH–OSiEt}_3,\ \text{ZnBr}_2]{\text{Aldol-GTP}}$ H/CH$_3$CO–[O–(CH$_2$)$_5$–C(=O)]$_m$–O–**R**–C(H)(OSiEt$_3$)–CH(OSiEt$_3$)$_n$–CH=O
**PCL-*b*-PVOTES (III)**

(**III**) $\xrightarrow[\text{THF, MeOH, HCl(1N,aq)}]{\text{Desilylation}}$ H/CH$_3$CO–[O–(CH$_2$)$_5$–C(=O)]$_m$–O–**R**–C(H)(OH)–CH(OH)$_n$–CH=O
**PCL-*b*-PVA**

**Scheme 1.** Route to PCL-*b*-PVA copolymer starting from the bifunctional initiator 4-HEBA.

molecular weights lower than 10000.[10] The biodegradation rate and various physical properties of PCL may be simultaneously adjusted and improved by the copolymerization of $\varepsilon$-CL with ethylenoxide.[11]

Water soluble poly(vinyl alcohol) (PVA) attracted our attention owing to its excellent properties, such as biodegradability, biocompatibility, hydrophilicity, high flexibility and good oxygen barrier. PVA theoretically has the potential of forming hydrogen bonding with oxygen atoms of the ester group. In fact, PVA is often chosen in research of biodegradable polymer blends to improve the brittle and hydrophobic properties of polyesters. The morphology and miscibility of PVA blended with other biodegradable polymers, for example, PCL, PLLA, etc., have been reported.[5,12] David *et al.*[13] investigated the biodegradation of PCL/PVA blend system and found these blends, even PCL rich, not to degrade by microorganisms from a compost of house-hold refuse, while pure PCL film was completely assimilated over 600–800 h.

We have developed a novel route to prepare PCL-*b*-PVA copolymers, where we took advantage of a bifunctional initiator, 4-(2-hydroxyethoxy)benzaldehyde (4-HEBA).[14] This initiator bears hydroxyl and formyl end groups responsible to ROP of $\varepsilon$-CL and aldol-type group transfer polymerization (Aldol-GTP) of triethylvinyloxylsilane as a precursor of PVA unit, respectively. This work puts emphasis on investigation of morphology and biodegradability of the PCL-*b*-PVA copolymers prepared by the above method. The results are useful to devise new applications of PCL-*b*-PVA copolymers.

## EXPERIMENTAL

### Materials

$\varepsilon$-CL was dried over CaH$_2$ and distilled under reduced pressure before use. Vinyloxytriethylsilane (VOTES) was synthesized as reported by Jung and Blum,[15] dried over CaH$_2$ for 24 h, and distilled under reduced pressure before use. 4-HEBA, stannous octanoate (Sn(Oct)$_2$), and acetyl chloride were commercially obtained in highly pure state and used without further purification. Zinc bromide (ZnBr$_2$) was purified by sublimation before use. Dichloromethane (CH$_2$Cl$_2$), diethyl ether (Et$_2$O), tetrahydrofuran (THF), triethylamine (Et$_3$N) and toluene were purified by distillation before use.

### Synthesis and Characterization

According to the route in Scheme 1, a novel PCL-*b*-PVOTES copolymer was synthesized using the bifunctional initiator 4-HEBA.

Sequence length of the two block components was determined by proton magnetic resonance spectroscopy ($^1$H NMR, Bruker DPX-200). Size-exclusion chromatograph (SEC, TSK HLC-803D system) in THF eluent was used to determine the molecular weight of PCL-*b*-PVOTES copolymer and its distribution, calibrated by polystyrene standards. PCL-*b*-PVA copolymer was reprecipitated from *n*-hexane after desilylation of PCL-*b*-PVOTES copolymer. The complete elimination of triethylsilyl groups was confirmed by $^1$H NMR monitoring. The formation of PCL-*b*-PVA copolymer was certified by a strong and broad peak at 3390 cm$^{-1}$ in its IR spectrum, which was assignable to hydroxyl groups of the newly generated PVA

block. With increasing PVA content, the block co-polymers became not sufficiently soluble in good solvents for PCL such as CHCl$_3$, THF, etc., but dissolved well in DMSO at 40 °C. Drastic change in solubility of the resulting copolymers is evidence for covalently bonding of the two block units. The added amount of MeOH and 1 N HCl aqueous solution (HClaq) should be controlled to avoid the hydrolysis of ester linkages in PCL block on occasion of desilylation. The degree of polymerization (DP) of PCL block after desilylation was determined by $^1$H NMR in DMSO and found to decrease with increasing HClaq. The polymerization route was convenient for preparing PCL-*b*-PVA copolymers having various molar ratios of two blocks.

### Preparation of PCL/PVA Blend

PCL homopolymer was synthesized according to the first step in Scheme 1. PVA homopolymer was prepared in this work by way of desilylation of PVOTES homopolymer ($M_n = 2.80 \times 10^3$, $M_w/M_n = 1.35$) synthesized through Aldol-GTP of VOTES in the presence of 4-HEBA as initiator. The PCL/PVA blend sample was obtained by dissolving two homopolymers in DMSO at 40 °C, stirring the mixture for 24 h, removing the solvent at 40 °C under reduced pressure, and drying *in vacuo* until constant weight. The PCL/PVA blend sample was granular.

### Thermal Analysis

Thermal analysis of PCL-*b*-PVA copolymer was carried out using DSC 210 (Seiko Instruments Inc.) in sealed aluminum pan under nitrogen flux. DSC thermal diagram for about 5 mg of sample was recorded from −130 to 220 °C at a heating rate of 10 °C min$^{-1}$ (the first heating scan). After rapid quenching, the sample was heated again from −130 to 220 °C at 20 °C min$^{-1}$ (the second heating scan). Melting point ($T_m$) was determined as the main peak top of the endothermic curve and heat of fusion ($\Delta H_m$) was estimated as the integral of the endothermic curve. Weight percent crystallinity was calculated assuming values of 136 and 152 J g$^{-1}$ for the complete crystalline PCL and PVA samples, respectively. Glass transition temperature ($T_g$) was determined as the midpoint of heat capacity change in the second DSC trace.

### Polarized Optical Microscopy (POM)

Polarized optical microscopic observation was done at room temperature using an OPTIPHOT2-POL model optical microscope equipped with a camera (UFX-II, Nikon Corp.). The sample film for POM measurement was cast on a glass plate with diameter of 16 mm.

### Biochemical Oxygen Demand (BOD) Test

Biochemical oxygen demand (BOD) for the polymeric sample in the presence of activated sludge was determined in duplicate using a BOD tester (Model 200F, TAITEC Corp.) by the oxygen consumption method and basically according to JIS K 6950 at 25 °C. Activated sludge was obtained from the municipal disposal plant at Meito-ku in Nagoya. The incubation medium was as follows (mg L$^{-1}$): K$_2$HPO$_4$, 217.5; KH$_2$PO$_4$, 85.0; Na$_2$HPO$_4$·2H$_2$O, 334.0; NH$_4$Cl, 5.0; CaCl$_2$·2H$_2$O, 36.4; MgSO$_4$·7H$_2$O, 22.5; FeCl$_3$·6H$_2$O, 0.25 (pH = 7.4). The concentration of polymer in the incubation medium was 100 mg L$^{-1}$. On bottom of test vessel, the film was cast from 10 mg polymer dissolved in 20 mL CHCl$_3$ and then evaporating CHCl$_3$ at room temperature for 3 d. The particle form of the sample was prepared by pulverization of the polymer concentrated from CHCl$_3$ solution. Biodegradability of the test substance was corrected by subtracting BOD for the blank from that of test solution and dividing it by theoretical oxygen demand (TOD) of the test substance. The induction period was defined as time when BOD corrected by that of the control blank reached 10% of TOD.

## RESULTS AND DISCUSSION

### Thermal Properties of PCL-b-PVA Copolymer

Because of the importance of morphology in biodegradability of a polymer, melting and crystallizing behavior of PCL-*b*-PVA copolymers bearing different block length ratios was first investigated by DSC measurement. The PCL homopolymer and the PCL/PVA blend containing 17 mol % PVA were used as reference samples. Although PVA is a biodegradable synthetic polymer, its biodegradability under natural environment is very poor. The biodegradability of PCL/PVA blends has already been reported by David *et al.*[13] According to their report, PCL/PVA blends are not degraded by microorganisms from a compost of household refuse, even though PCL rich. Consequently there must be a certain upper limit for PVA content in PCL-*b*-PVA copolymers to ensure these copolymers as practical biodegradable materials. PVA content in the block copolymers was adjusted to be below 30 mol %.

As shown in Table I, the thermal properties of PCL-*b*-PVA copolymers, PCL homopolymer, and PCL/PVA blend were determined from the second heating in DSC measurement after removing effects due to different thermal histories of samples through the first scanning. Figure 1 illustrates DSC thermograms of PCL-*b*-PVA copolymers with different PCL/PVA molar ratios. If two components are miscible well in the amorphous region, only one glass tran-

**Table I.** Thermal properties of PCL-*b*-PVA copolymers and PCL homopolymers[a]

| No. | $DP_{PCL}/DP_{PVA}$[c] | PCL/PVA[d] (mol/mol) | $T_g$ (°C) | $T_m$ (°C) | $\Delta H_f$ (J g$^{-1}$) | $X_c$ (%) |
|---|---|---|---|---|---|---|
| 1 | 67/0 | 100/0 | −75.4 | 53/56 | 74.7 | 54.9 |
| 2 | 68/7 | 91/9 | −73.8 | 49/52 | 70.5 | 53.3 |
| 3 | 67/9 | 88/12 | −83.1 | 52.8 | 70.8 | 54.8 |
| 4 | 72/12 | 86/14 | −51.3 | 52.5 | 66.1 | 51.7 |
| 5 | 75/19 | 80/20 | −86.1 | 52.2 | 71.3 | 57.5 |
| 6 | 55/0 | 100/0 | −70.7 | 52/55 | 76.5 | 56.3 |
| 7 | 60/17 | 78/22 | −94.6 | 52.8 | 61.7 | 50.3 |
| 8 | 56/19 | 75/25 | −78.8 | 53.3 | 66.9 | 55.5 |
| 9 | 31/0 | 100/0 | −66.6 | 50/54 | 83.0 | 61.0 |
| 10 | 36/14 | 72/28 | −93.0 | 52.8 | 55.7 | 52.2 |
| 11 | 46/0 | 100/0 | −74.9 | 50/55 | 81.9 | 60.2 |
| 12[b] | 46/17 | 83/17 | −87.3 | 51/55 | 75.4 | 59.8 |

[a]Measured by DSC at second heating scan (20 °C min$^{-1}$). [b]PCL/PVA blend. [c]Degrees of polymerization (DP) of PCL and PVA block determined by $^1$H NMR. [d]Molar ratio of PCL and PVA block in the block copolymers.
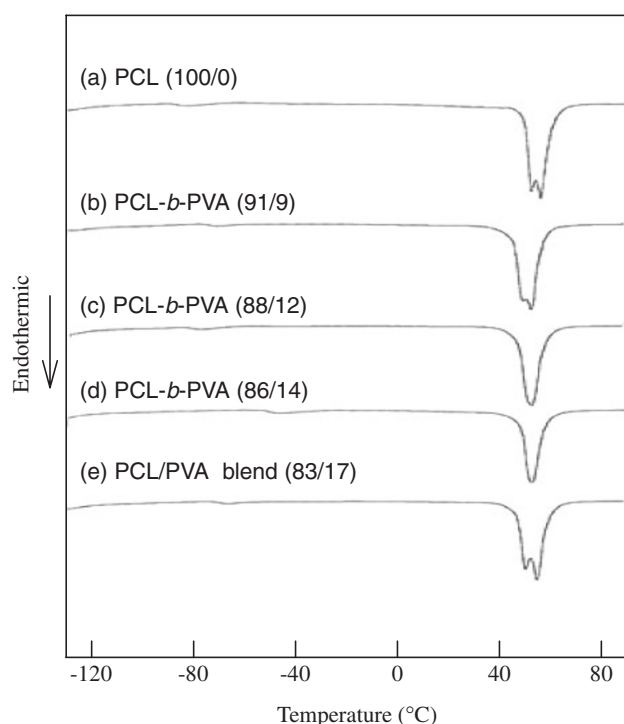


**Figure 1.** DSC thermal diagrams of PCL-*b*-PVA copolymers, PCL homo-polymer, and PCL/PVA blend by the second heating scan (20 °C min$^{-1}$).

sition temperature ($T_g$) usually appears in DSC thermograms at an intermediate temperature between $T_g$s of two pure homopolymers. Even if two components are partially miscible, $T_g$ of each component should be affected by each other, and usually be composition dependent, for example as Fox's equation. $T_g$ of PVA phase would lie in the melting range of PCL. $T_g$ due to PCL block moves toward lower temperature in comparison with the corresponding PCL homo-polymer except for sample 4, indicating that the two block components are immiscible in the amorphous

region for the composition range of our block copolymers. The compatibility of PCL-*b*-PVA copolymer is supposed to be affected by the sequence length of the two blocks.

Although an endothermic peak due to melting of PVA block was observed for a few samples at the first heating scan, no endothermic peak appeared for any sample at the second heating scan. It seems reasonable that the major PCL component suppresses the crystallization of the minor PVA component. Table I shows the degree of crystallinity of PCL block calculated by the following eq 1:

$$X_c = \Delta H_f/(\Delta H_f^0 w) \qquad (1)$$

where $\Delta H_f$ is the apparent enthalpy of fusion (indicated as melting enthalpy per gram in DSC thermograms), $w$ is the weight fraction of PCL block and $\Delta H_f^0$ is the enthalpy of fusion per gram of PCL block in the completely crystalline state.

No matter of their compositions, the PCL block in PCL-*b*-PVA copolymers showed lower $\Delta H_f$ than the PCL homopolymer having similar sequence length as the block copolymer. Except for sample 5 in Table I, the crystallinity of PCL block in PCL-*b*-PVA copolymer generally decreased in comparison with the PCL homopolymer, regardless of block length. Sample 5 contains 20 mol % PVA and shows a higher crystallinity than that of the PCL homopolymer. In the DSC measurement of the PCL homopolymer, a double endothermic peak for the melting was clearly observed (Figure 1a), indicating the presence of two distinguishable crystalline types for the PCL chain, possibly due to different degrees of ordering or size of crystallites. Such differences may arise from reorganization of crystal during DSC heating. In the DSC thermogram of the PCL-*b*-PVA copolymer containing 9 mol % PVA (Figure 1b), a similar double en-

dothermic peak for the melting derived from PCL block moving toward lower temperature was observed. For PCL-*b*-PVA copolymers having more than 12 mol % of PVA content (Figure 1c, d), the melting peak corresponding to PCL block was unimodal. The DSC thermogram of the PCL/PVA blend consisting of 17 mol % PVA showed a double melting peak at the same position (Figure 1e) as the pure PCL homopolymer (Figure 1a), indicating that the added PVA component in the blend does not yet influence the crystallization manner of PCL homopolymer.

For PCL-*b*-PVA copolymers, change of the melting peak corresponding to PCL block with increasing content of PVA block indicates that the crystallization manner of PCL block is greatly influenced by the covalently bonded PVA block. For the composition range in this work, it is very likely that the PVA block was finely dispersed in the continuous PCL phase.

*Effects of PVA Block on Morphology of PCL-b-PVA Copolymer as Observed by Polarized Optical Microscope (POM)*

To discuss the effects of PVA block on the crystallization manner of PCL block, the polarized optical microscopic image was taken for the solution-cast film on glass plate at room temperature. The surface morphology of the sample was influenced by the thickness of the film. A chloroform solution (7.5 wt %) of PCL-*b*-PVA copolymer was thus cast on a glass plate of 16 mm diameter so as to form a film with the same thickness.

Figure 2 shows POM-images of PCL-*b*-PVA copolymers with different compositions by only changing the sequence length of PVA block. The images of the corresponding PCL and PVA homopolymers are also shown in Figure 2. When pure PVA was cast on the glass, no spherulite was observed (Figure 2b). Thus, all spherulites observed for PCL-*b*-PVA copolymer originated from PCL block. As seen in Figure 2a, many spherulites with Maltese crosses and polygonal edges were observed for the PCL homopolymer. For the PCL-*b*-PVA copolymer having 9 mol % of PVA (Figure 2c, d), the ring banded-type spherulite limited by hyperbole branches is larger than that of the PCL homopolymer. With increasing PVA content to 12 mol %, the domain size of PCL crystallite was smaller compared with the PCL homopolymer. Many black spaces, which did not appear in the photograph of PCL homopolymer, were dispersed among the ring banded-type spherulites of PCL blocks. These black spaces can be ascribed to the PVA block region. The existence of PVA block may restrict the growth of the PCL crystallite, resulting in the formation of ring banded-type spherulites.

Two different images coexisted in the block copolymer composing of 20 mol % PVA as shown in Figure 2g and 2h. The molecular weight distribution of PCL-*b*-PVA copolymer was somewhat broadened after desilylation even though effort was made to suppress unfavorable side reactions by controlling the amount of HClaq. With increasing block length of PVA, block copolymers with different block lengths due to the broad molecular weight distribution may have distinct solubility in CHCl$_3$, resulting in different crystalline zones.

The size of spherulite may be reduced by increasing PVA content. It was verified through POM images of block copolymers of constant block length of PVA and different block lengths of the PCL component. By increasing PVA content from 20 to 28 mol %, the resulting block copolymer did not dissolve in good solvents for PCL homopolymer, but dissolved in DMSO at 40 °C. Therefore, the film cast on the glass plate from DMSO solution at 40 °C and dried *in vacuo* was examined. As shown in Figure 3, the increment of PVA block may result in very fine and unmeasurably small spherulites. The amorphous PVA blocks bonded with the crystalline PCL blocks may act as nucleation agent, generating a great number of seeds for crystallization. Crystallites grew within a limit space, resulting in building up small spherulites. The amorphous PVA block covalently bonded with PCL block may thus be dispersed in the crystalline phase of PCL and influence the crystallization manner of PCL block.

*Effects of Polymer Shape on Biodegradability of PCL-b-PVA Copolymer*

The biodegradation of PCL-*b*-PVA copolymers was estimated by monitoring biochemical oxygen demand (BOD) of samples in the presence of activated sludge.

The biodegradation rate of PCL homopolymer depends on the surface area since the biodegradation is thought to proceed from the surface of polymer.[16] Under the conditions in this work, the same was confirmed, as seen in Figure 4. Two PCL samples were prepared. The first was directly cast from CHCl$_3$ solution on bottom of test vessel (■) and the second with lower molecular weight was used as particles in shape (▲). Both showed very similar induction periods in the BOD test, but the latter attained lower BOD/TOD value (about 60% as an average) after 40 d. Thus, the influence of polymer shape on the biodegradability of PCL-*b*-PVA copolymer was investigated in detail. Figure 4 shows biodegradation curves for the PCL-*b*-PVA copolymer containing 14 mol % PVA in different shapes. As summarized in Table II, the sample film prepared by solvent-cast on bottom of test vessel (×) began to degrade at 13 d and BOD/TOD reached 75% at 40 d. For the same sample as particles (○), a longer induction period was required and
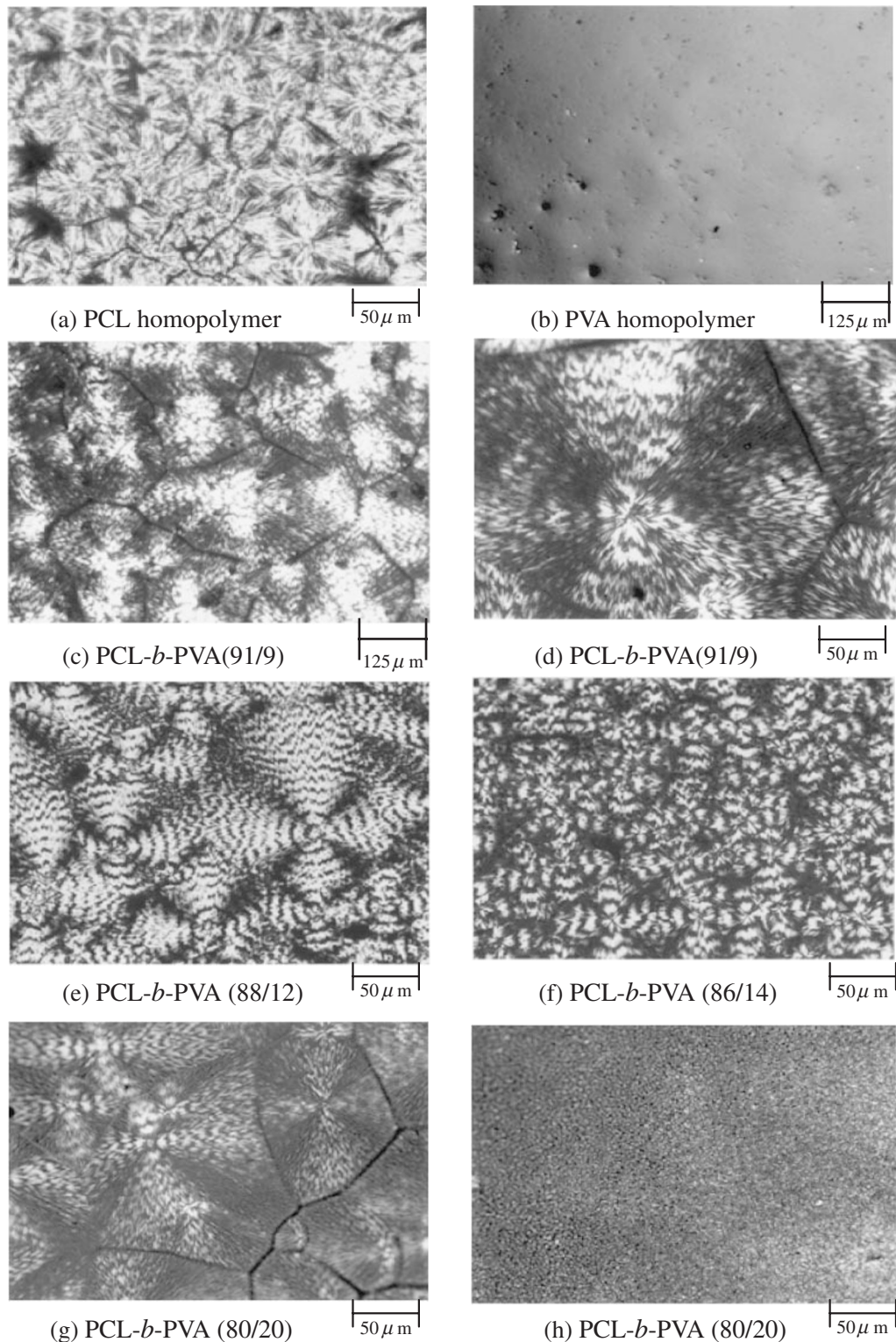
**Figure 2.** Polarized optical micrographs of PCL-*b*-PVA copolymers, PCL, and PVA homopolymer as listed in Table I, at room temperature.

BOD/TOD at 40 d decreased. The biodegradation curve of the film (10 mm × 10 mm, 67–100 μm thick) (◆) removed from a Teflon plate after solvent evaporation showed a longest induction period of 24 d and 48% BOD/TOD at 50 d, indicating that biodegradation was affected by surface area and thickness of the film. The fastest biodegradation rate of the sample cast on bottom of test vessel must be reflected by the widest surface area and least thickness. Similar to the PCL homopolymer, increased surface area of the block copolymer promoted biodegradability.

**Table II.** Induction periods and biodegradability at 40 d based on BOD curves for PCL-*b*-PVA (86/14) in different shapes as shown in Figure 4

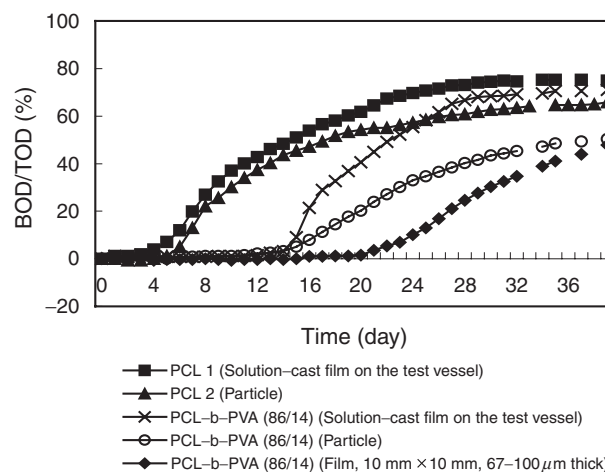| Sample[a] | $DP_{PCL}/DP_{PVA}$[b] | Induction period[c] (d) | BOD/TOD (%) at 40 d |
|---|---|---|---|
| PCL 1 (100/0) (solution-cast film on the test vessel) | 74/0 | 6 | 73.5 |
| PCL 2 (100/0) (particle) | 46/0 | 7 | 59.5 |
| PCL-*b*-PVA (86/14) (solution-cast film on the test vessel) | 72/12 | 14 | 75.0 |
| PCL-*b*-PVA (86/14) (particle) | 72/12 | 17 | 50.4 |
| PCL-*b*-PVA (86/14) (film, 10 mm × 10 mm, 67–100 μm thickness) | 72/12 | 24 | 47.8 (50 d) |

[a]( ) shows molar ratio of PCL and PVA block in PCL-*b*-PVA copolymer, as determined by ^{1}H NMR. [b]Degrees of polymerization (DP) of PCL and PVA block determined by ^{1}H NMR. [c]Time needed for biodegradation to reach 10% theoretical value.
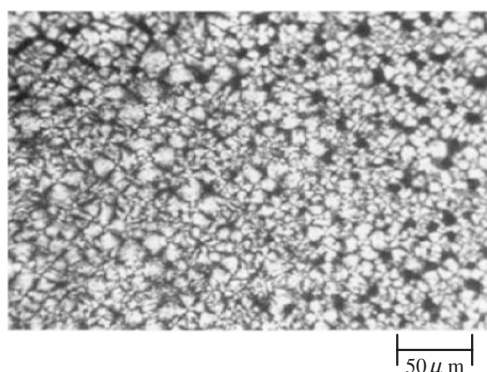


**Figure 3.** Polarized optical micrograph of PCL-*b*-PVA (75/25) copolymer at room temperature.



**Figure 4.** Biochemical oxygen demand (BOD) test of PCL-*b*-PVA (86/14) copolymer in different shapes.
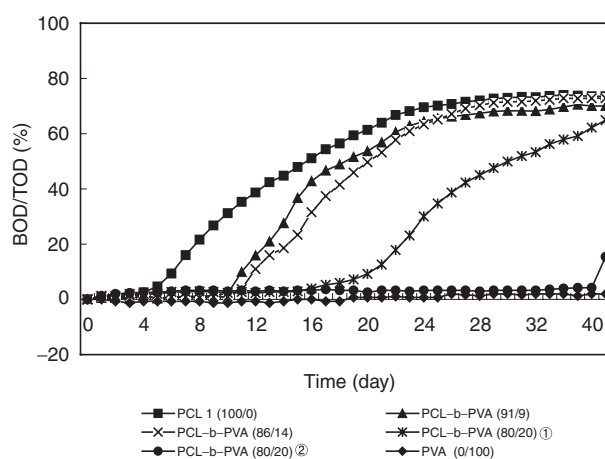


**Figure 5.** Biochemical oxygen demand (BOD test of PCL-*b*-PVA copolymers prepared by solvent-cast on bottom of test vessel.

*Effects of PVA Content on Biodegradability of PCL-b-PVA Copolymer*

The shape of the block copolymer is an important factor of biodegradability. The effect of PVA content on the biodegradability of PCL-*b*-PVA copolymers with changing only sequence length of PVA block was examined for same shape samples as prepared by casting on bottom of test vessel from CHCl$_3$ solution. The biodegradability of PVA and PCL homopolymer was examined under the same conditions. Figure 5 shows BOD/TOD plotted against reaction time. In the present work, BOD for the PVA homopolymer (◆) never exceeded 6% of the theoretical value (TOD) even at 47 d. Microorganisms in the activated sludge thus do not assimilate PVA well, although the degradation of PVA by other stains has been reported.[17] The biodegradation of PCL homopolymer (■) began after 6 d and BOD/TOB reached to 73% at 47 d. Therefore, the PCL block must be mainly responsible for the biodegradation of PCL-*b*-PVA copolymer.

As summarized in Table III, the induction period

for block copolymer was prolonged with increasing PVA content. The existence of PVA block may inhibit microorganisms from moving toward the PCL block region. In spite of the prolonged induction period,

**Table III.** Induction periods and biodegradability at 46 d based on BOD curves
for PCL-*b*-PVA copolymers as shown in Figure 5

| Sample[a] | DP$_{PCL}$/DP$_{PVA}$[b] | Induction Period[c] (d) | BOD/TOD (%) at 46 d |
|---|---|---|---|
| PCL 1 (100/0) | 74/0 | 6 | 73.5 |
| PVA (0/100) | 0/17 | —[d] | 5.8 |
| PCL-*b*-PVA (91/9) | 68/7 | 11 | 70.1 |
| PCL-*b*-PVA (86/14) | 72/12 | 12 | 72.9 |
| PCL-*b*-PVA (80/20) | 75/19 | 21 (46) | 64.9 (15.4) |

[a]( ) shows molar ratio of PCL and PVA blocks in PCL-*b*-PVA copolymers determined by ^{1}H NMR. All samples were prepared by solvent-cast on bottom of test vessel. [b]Degrees of polymerization (DP) of PCL and PVA block evaluated by ^{1}H NMR. [c]Period needed for biodegradation to reach 10% theoretical value. [d]No decomposition.

**Table IV.** Induction periods and the biodegradability at 47 d based on BOD curves
for PCL-*b*-PVA copolymers as shown in Figure 6

| Sample[a] | DP$_{PCL}$/DP$_{PVA}$[b] | Induction Period[c] (d) | BOD/TOD (%) at 47 d |
|---|---|---|---|
| PCL 2 (100/0) | 46/0 | 6 | 59.8 |
| PCL-*b*-PVA (80/20) | 75/19 | 16 | 34.5 |
| PCL-*b*-PVA (78/22) | 60/17 | 15 | 55.5 |
| PCL-*b*-PVA (75/25) | 56/19 | —[d] | — |
| PCL-*b*-PVA (72/28) | 36/14 | —[d] | 6.1 |

[a]( ) shows molar ratio of PCL and PVA blocks in PCL-*b*-PVA copolymers determined by ^{1}H NMR. All samples were examined in a shape of particles. [b]Degrees of polymerization (DP) of PCL and PVA block evaluated by ^{1}H NMR. [c]Period needed for biodegradation to reach 10% theoretical value. [d]No decomposition.

the biodegradation rate for the block copolymer after the induction period is faster than that for the pure PCL, which may be ascribed to lower crystallinity in the block copolymer. Similar accelerated rates are mentioned in biodegradation of PCL/PEG block copolymers.[18] BOD/TOD data were generally obtained in good reproducibility and are shown as average values in the last column in Table III except for the block copolymer having 20 mol % PVA (∗, ●). The non-reproducible biodegradation data for this sample might be related to the two different morphology states observed in the POM image since the biodegradation manner can be affected by morphology. Thus, longer induction period and slower degradation rate are brought about in biodegradation when more homogenously the PVA segment disperses in the PCL matrix.

With increasing content of PVA block, the block copolymer did not dissolve in CHCl₃, but dissolved in DMSO at 40 °C. Considering that traces of DMSO are harmful for microbial degradation, BOD test for all samples was examined in the shape of particles. As shown in Figure 6, in the case of PCL-*b*-PVA copolymer composed of PVA blocks having same sequence length while the content of PVA blocks increased from 20 mol % (∗) to 25 mol % (|), the biodegradation of the block copolymer was suppressed during observation. For the biodegradable samples, the induction periods were similar no matter
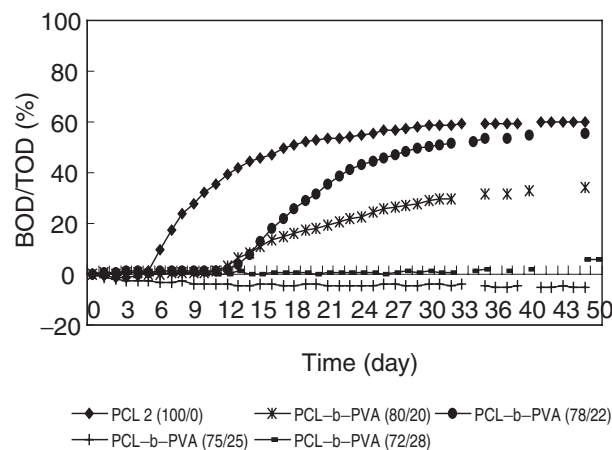


**Figure 6.** Biochemical oxygen demand (BOD) test of PCL-*b*-PVA copolymers in a shape of particles.

of the PVA contents, while the degree of biodegradation decreased with increasing PVA content as shown in Table IV. The relatively high degradation rate of block copolymer with 22 mol % PVA (●) may be ascribed to comparatively low crystallinity.

*Comparison of Biodegradability for the PCL Homopolymer, PCL/PVA Blend, and PVA Homopolymer*

We examined the biodegradability of the blend of PCL with PVA through BOD test in the presence of activated sludge. The BOD test for the PCL/PVA
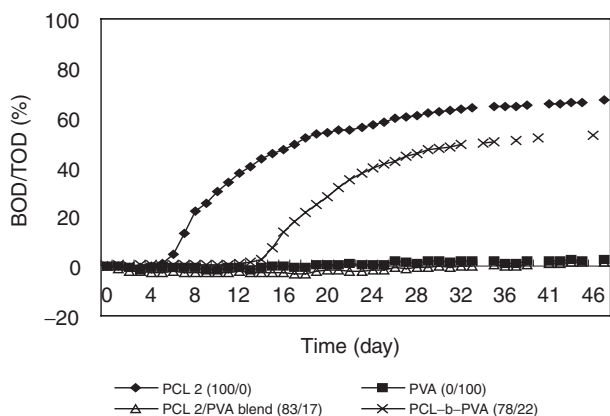
**Figure 7.** Biochemical oxygen demand (BOD) test of PCL homopolymer, PCL/PVA blend, PCL-*b*-PVA copolymer, and PVA homopolymer.



**Figure 8.** Biochemical oxygen demand (BOD) test of PCL homopolymer and simple mixture of PCL and PVA homopolymers (not blend).

blend (83/17 mol/mol) (△) did not show biodegradation even at 47 d. However, the biodegradation of PCL-*b*-PVA copolymers having 17–22 mol % PVA content took place though a long induction period was required. Poor biodegradability of the blend is rather similar to that of PVA homopolymer (Figure 7).

David *et al.*[13] maintained that the PVA homopolymer in the blend is dissolved into the culture medium and then covered on the PCL layer to make a protective film, which effectively obstructs the biodegradation of the PCL homopolymer. No occurrence of biodegradation for the simple mixture of PCL and PVA homopolymers (not blend) furthermore supports this, as shown in Figure 8 (▲).

In contrast, the PVA component in the block copolymer may never dissolve in the culture medium because it is covalently bonded to PCL block. PVA blocks must exist over the crystalline and amorphous regions of PCL component. Even though PVA blocks effectively prevent the degradation of PCL-*b*-PVA copolymers with microorganisms, the degradation of the block copolymers may still occur so far as the PVA content is below 25 mol %. The biodegradation rate of PCL-*b*-PVA copolymer may thus be optionally adjusted by changing the sequence length of the two blocks.

## CONCLUSIONS

The morphology of PCL-*b*-PVA copolymers (PVA content: 9–28 mol %) was investigated through DSC and POM measurements. The two blocks were immiscible in amorphous region, the PVA block was always amorphous state, and the PVA block influenced the crystallizing manner of PCL block, as shown by the conspicuous change in spherulite structure due to the PCL block. The PVA segment was dispersed in the
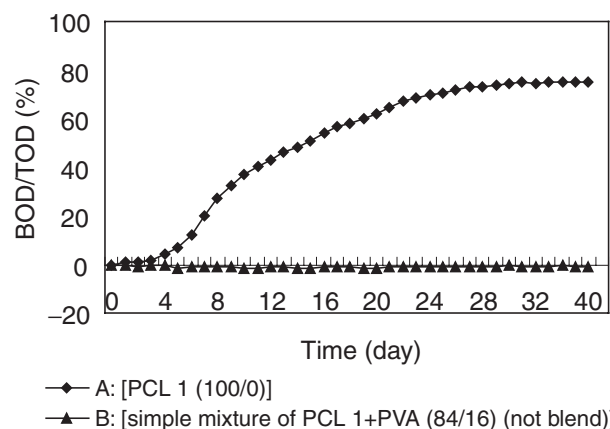
matrix of PCL as seen in POM images. The size of spherulite decreased with increasing PVA content. The PVA block bonded covalently to the PCL block acts as nucleation agents in the PCL matrix. Thus, a great number of nucleuses generated from the nucleation agents simultaneously grow in a limited space to form small spherulites.

The same shape of PCL-*b*-PVA samples for BOD test is required to compare correctly the data. The biodegradation of PCL-*b*-PVA copolymers was shown to actually take place only at the PCL block moiety. Compared with PCL homopolymer, the biodegradability of PCL-*b*-PVA copolymer was reduced with increasing content of PVA block. When the content of PVA in the block copolymers exceeded 25 mol %, no biodegradation occurred within the period set in this study. Differing from the blending system of PCL and PVA, our PCL-*b*-PVA copolymer makes controlling biodegradation rate possible. It is caused by the fact that two components are covalently bonded.

## REFERENCES

1. M. Ohrlander, R. Palmgren, A. Wirsen, and A. C. Aibertsson, *J. Polym. Sci., Part A: Polym. Chem.*, **37**, 1659 (1999).
2. N. Kumagai and Y. Doi, *Polym. Degrad. Stab.*, **36**, 241 (1992).
3. A. Lisuardi, A. Schoenberg, M. Gadaa, R. A. Gross, and S. P. McCarthy, *Polym. Mater. Sci. Eng.*, **67**, 298 (1992).
4. Y. S. Chun and W. N. Kim, *Polymer*, **41**, 2305 (1999).
5. C. D. Kesel, C. Lefevre, J. B. Nagy, and C. David, *Polymer*, **40**, 1969 (1999).
6. H. Tsuji and T. Ishizaka, *Int. J. Biol. Macromol.*, **29**, 83 (2001).
7. J. K. Kim, D. J. Park, M. S. Lee, and K. S. Ihn, *Polymer*, **42**, 7429 (2001).
8. L. Tao, B. Luan, and C. Y. Pan, *Polymer*, **44**, 1013 (2003).

9. Y. K. Choi, Y. H. Bae, and S. W. Kim, *Macromolecules*, **31**, 8766 (1998).

10. S. H. Lee, S. H. Kim, Y. K. Han, and Y. H. Kim, *J. Polym. Sci., Part A: Polym. Chem.*, **40**, 2545 (2002).

11. S. G. Wang and B. Qiu, *Polym. Adv. Technol.*, **4**, 363 (1993).

12. X. T. Shuai, Y. He, N. Nakashima, and Y. Inoue, *J. Appl. Polym. Sci.*, **81**, 762 (2001).

13. C. D. Kesel, C. V. Wauven, and C. David, *Polym. Degrad. Stab.*, **55**, 107 (1997).

14. J. Zhou, A. Takasu, Y. Inai, and T. Hirabayashi, *Polym. J.*, **36**, 182 (2004).

15. M. E. Jung and R. B. Blum, *Tetrahedron Lett.*, **43**, 3791 (1977).

16. Y. Doi, Y. Kanesawa, M. Kunioka, and T. Saito, *Macromolecules*, **23**, 26 (1990).

17. T. Suzuki, *J. Appl. Polym. Sci.: Appl. Polym. Symp.*, **35**, 431 (1979).

18. M. Yuan, Y. Wang, X. Li, C. Xiong, and X. Deng, *Macromolecules*, **33**, 1613 (2000).